Astron. Astrophys. 318, 565–570 (1997)

ASTRONOMY AND ASTROPHYSICS

Burnham's nebula (HH 255), a peculiar Herbig-Haro object

K.H. Böhm[1,⋆] **and J. Solf**[2]

[1] Department of Astronomy, Box 351580, University of Washington, Seattle, WA 98195, USA (e-mail: bohm@astro.washington.edu)
[2] Thüringer Landessternwarte Tautenburg, Sternwarte 5, D-07778 Tautenburg, Germany (e-mail: solf@tls-tautenburg.de)

Received 26 March 1996 / Accepted 27 June 1996

Abstract. Burnham's nebula (HH 255) has been consistently identified as a Herbig-Haro object, i.e. a radiating shock wave. Spectrophotometry shows that at least a considerable part of this shock wave must have a velocity of ∼90 km s^{-1} or more. Recently, position-velocity diagrams have shown that the centroid radial velocity and the radial velocity dispersion are unusually small in HH 255 causing problems in the detailed shock wave interpretation. A bow shock like structure is excluded.

In order to get some insight into the physics of this enigmatic HH object we have studied the degree of ionization, the kinematic state and the electron density as a function of position near the main axis of HH 255. We find that the ionization (visible in a steep increase in O^{++}, N^{+} ions and in a decrease in C° and Ca^{+}) occurs in a very narrow ($1\farcs0$ – $1\farcs5$ wide) region which is centered at ∼3″ S of T Tau. In the same narrow region the centroid radial velocity drops rapidly to zero and the radial velocity dispersion has a maximum and then drops rapidly to 25 km s^{-1} (FWHM). Beyond $4\farcs5$ S of T Tau HH 255 looks *qualitatively* like a pure recombination zone. The [O III] lines and then the [N II] lines become gradually weak in comparison to neutral and low-ionization lines. However, this interesting region, which forms the bulk of HH 255, is about 100 times wider than the theoretical prediction for the recombination region of a plane shock with the same post-shock density and the same shock velocity as HH 255. Consequently an interpretation of the zero radial velocity region as a plane shock seen edge-on is also excluded.

Key words: stars: individual: T Tau – stars: pre-main sequence – ISM: individual: Burnham's nebula – ISM: jets and outflows – ISM: kinematics and dynamics

1. Introduction

A method to learn more about the origin of jets from T Tauri stars is the study of the circumstellar velocity (especially in forbidden lines) as close to the star as possible. An approach developed by Solf (1989) uses long-slit spectra going through the star, but it eliminates the radiation from the stellar photosphere by using the radiation of a star of equal spectral type as a template in the spectral range of the studied line. The method yields detailed position-velocity diagrams of the circumstellar matter.

The procedure has been applied successfully to the environment of a number of active T Tauri stars (Solf 1989, 1993; Solf & Böhm 1993; Hirth et al. 1994; Böhm & Solf 1994; Hirth 1994, see also Staude & Elsässer 1993). The interesting results for most stars are partially in agreement with the theoretical predictions by Kwan & Tademaru (1988, 1995).

In comparison to the conclusions drawn for other T Tauri stars the study of T Tau itself (Böhm & Solf 1994) leads to a number of unexpected results which still have to be interpreted. Whether these results are strongly influenced by the fact that T Tau is a binary star is not yet clear.

There are two basic results for the circumstellar environment of T Tau which differ from those for other active T Tauri stars. 1) In the immediate environment of T Tau one can clearly detect two different systems of outflows. (In other T Tauri stars one sees only one system.) The first one has the position angle (P.A.) 270° (counter jet not detected, see Schwartz 1975; Bührke et al. 1986) and the other system with the P.A. 165°/345°. 2) At distances of ∼$3\farcs5$ to ∼11″ (best seen at P.A. 180°, but visible at least between P.A. 135° and 225°) there is a spatio-kinematic component E (identified by Böhm & Solf 1994, see Fig. 1) which corresponds to the main part of Herbig-Haro object HH 255 (Reipurth 1994) and which is related to the main part of Burnham's (1894) nebula. The component E shows enigmatic kinematic properties. Both results 1) and 2) are unexpected and very important. In the present *paper*, however, we shall restrict ourselves only to the discussion of point 2.

In a way the existence of Burnham's nebula, which seems to show an HH spectrum and is somehow connected with T Tau, has been considered an enigma for a long time (see, e.g., Herbig 1950, 1951; Osterbrock 1958; Schwartz 1974). However, only the recent determination of the position-velocity diagrams of HH 255 which we identify with the main part of Burnham's nebula (Böhm & Solf 1994) have shown us how difficult the problem

Send offprint requests to: J. Solf

⋆ Research was carried out in part during a visit to the Thüringer Landessternwarte Tautenburg

really is. We found that the environment of T Tau consists of two rather different subregions. First the immediate neighborhood of the star shows (as mentioned) the formation of the two systems of outflows. It has large velocity dispersions and in general also large centroid radial velocities. Kinematically very different is the southern part of the T Tau environment which is identified with component E. Böhm & Solf (1994) found the following kinematic properties for this main part of HH 255. The centroid velocity lies mostly in the range 0 km s^{-1} to -3 km s^{-1} (with respect to the star) and the velocity dispersion (FWHM) has a value of only $\sim$25 km s^{-1}. (The centroid velocity and the velocity dispersion have been derived by means of a gaussian line fit to the observed line profiles.) Both the low velocity dispersion and the centroid velocity which is practically indentical to the star cause serious problems to construct a consistent model of a HH shock wave with (at least) 90 km s^{-1} shock velocity required by the line fluxes.

In the following brief *paper* we shall try to obtain more useful information about the physical conditions in Burnham's nebula especially in component E (Fig. 1). These include the centroid radial velocities, the radial velocity dispersion, the electron density, and especially the ionization, which may contain the important clue to understanding of Burnham's nebula. The hope is that the additional information about these physical parameters will give us more insight into the physics of HH 255 and eventually will make this enigmatic object more understandable.

2. Observations

The observational results which have been used in this *paper* can be extracted from earlier observations which have been discussed by Solf et al. (1988) and Böhm & Solf (1994). The first observations were carried out on December 6 and December 8, 1986 with the 3.5–m telescope at the Calar Alto Observatory (Spain) using the Cassegrain Spectrograph in the echellette mode with an RCA CCD detector. The spectral and spatial resolutions are about 100 km s^{-1} and $1''$, respectively. These observations are mainly used for the comparison of different line ratios. The second observations which we used mostly for the determinations of the velocity dispersion, the centroid radial velocity and in part for the determination of the ionization were carried out on August 14–18, 1992 with the 2.2–m telescope at the Calar Alto Observatory. The long-slit spectra ($117''$) were obtained with the f/12 camera of the coudé spectrograph. The spectral and the spatial resolutions are 10 km s^{-1} and $1''.0 - 1''.3$, respectively. The detector was a Tektronix CCD with 1024×1024 pixels.

In both sets of observations the photospheric spectrum of T Tau has been eliminated. In the long-slit coudé spectra the elimination of the photospheric radiation has been carried out with Solf's (1989) method in which the K0 IV star η Cep has been used as a template. More detailed information about the observations is given by Solf et al. (1988) and by Böhm & Solf (1994).

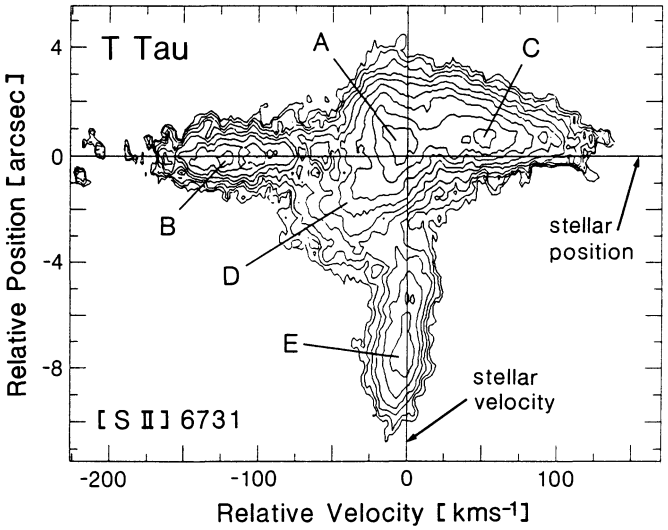

Fig. 1. The position-velocity diagram for the line [S II]λ6731 in the environment of T Tau for P.A. 0°. The diagram shows the definition of the different spatio-kinematic components. Component E is the main part of HH 255. See also Böhm & Solf (1994).

3. Results

In the following we use for the definition of the different spatio-kinematic regions of the circumstellar environment of T Tau the position-velocity diagram of the line [S II]λ6731 at P.A. 0° (Fig. 1). These regions are also recognizable in the position-velocity diagrams of [O I]λ6300 and [N II]λ6583 although there are some quantitative differences (Böhm & Solf 1994). For the following investigation it is considered as important that Burnham's nebula is an HH object (Herbig 1950, 1951; Osterbrock 1958; Schwartz 1974; Solf et al. 1988) and consequently forms a shock wave.

In order to obtain further insight into the apparent contradiction between the shock wave character of HH 255 and the extremely low radial velocity and velocity dispersion mentioned in the *Introduction* we study first the ionization in HH 255. Later we shall try to establish a relation between the ionization and the kinematic properties.

We will explore the region south of T Tau (where most of the emission of HH 255 occurs). In this region the distributions of physical quantities are influenced by components D and E (and to a lesser extent by A). We are mainly interested in component E, but the possible physical connection between D and E will be of great interest.

In Fig. 2 we show a number of empirical ionization indicators as a function of the distance from T Tau. These are the line intensity ratio [N II]λ6583/[O I]λ6300 as well as the intensities of [O III]λ5007, [Ca II]λ7291 and [C I]λ9850. The line intensity ratio [N II]λ6583/[O II]λ6300 is basically an ionization criterion because the excitation for both lines shows considerable similarities (Böhm & Solf 1994) and, therefore, any drastic changes must be due to changes in ionization. Moreover, the ionization potentials of O° and N° are similar (13.62 eV and 14.53 eV). Finally, the empirically determined electron density changes very

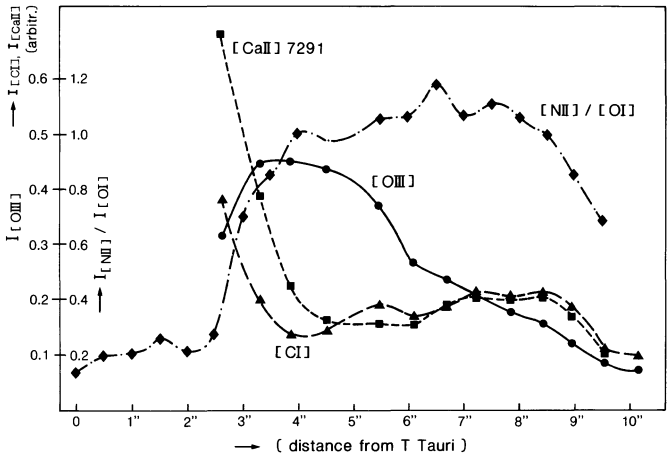

Fig. 2. Variation of line intensities [O III]λ5007, [C I]λ9850, [Ca II]λ7291 and the line ratio [N II]λ6583/[O I]λ6300 (which are indicators of ionization changes, see text) as a function of the distance from T Tau for P.A. 180°. All curves point towards a rapid increase of the ionization at $\sim$3″ and a slow recombination in the interval 4″–10″. The intensities for the [O III], [Ca II], and [C I] are plotted on an arbitrary scale. The estimated relative error for the [N II] and [O I] intensities is $\pm$5%, for the [OIII] intensity $\pm$10%, and for the [Ca II] and [C I] intensities $\pm$15–20%.

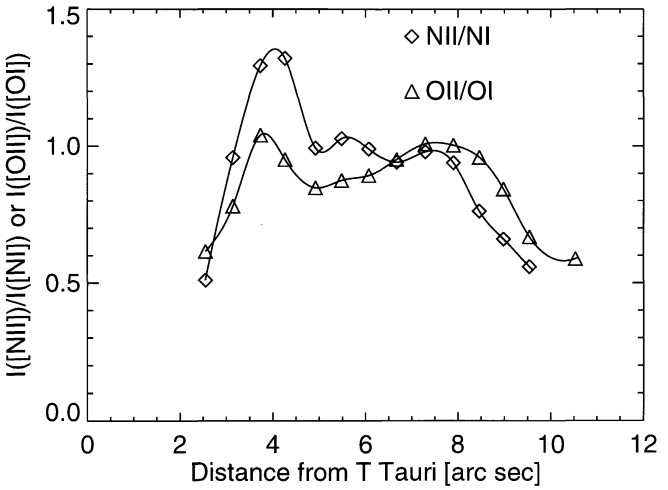

Fig. 3. Variation of the line intensity ratio [O II]$\lambda\lambda$(3726 + 3729) / [O I]$\lambda\lambda$(6300 + 6363) and [N II]$\lambda\lambda$(6548 + 6583) / [N I]$\lambda\lambda$(5198 + 5200) as a function of distance from T Tau for P.A. 180°. These ratios are considered as crude secondary indicators of the ionization (see text). The estimated relative error for the [O I] and [N II] intensites is $\pm$5%, for [O II] and [N I] about $\pm$15 %.

little in the whole spatial range considered (from 2″ to 10″; see below, Fig. 6) and it is consequently difficult to imagine that the excitation would change over a short distance.

The [O III]λ5007 line strength changes drastically in HH objects and that is always attributed to a change in ionization (Raga & Böhm 1985, 1986; Hartigan et al. 1987). While the great strength of [O III] is an indicator of high ionization, the strength of [CI]λ9850 (ionization energy of C°: 11.26 eV) and [Ca II]λ7291 (ionization energy of Ca^+: 11.87 eV) are indicators of low ionization.

Fig. 2 shows a surprising result. At 3″ from T Tau all four curves show clearly a very steep increase of ionization (which goes at least up to O^{++}; requiring the ionization energy of O^+: 35.12 eV). The curve for the intensity ratio [N II]λ6583/[O I]λ6300 and the intensity curve for [O III]λ5007 rise very steeply whereas the intensity distribution for [C I]λ9850 and for [Ca II]λ7291 decrease steeply at the same place. It is remarkable how small the region is in which all these drastic ionization changes happen. With an extent of only $\sim$1″ the details are probably already influenced by the seeing and the change in the ionization may be even steeper than indicated in Fig. 2. In any case there can be little doubt that an abrupt and very strong increase of ionization occurs at $\sim$3″ south of T Tau. This is the region which is strongly influenced by component D, probably more than by E.

If we consider the properties of the ionization in the main part of component E (3.″5 – 10″) then we find a *qualitative* behavior like in a recombination zone. The O^{++} ions are already partially reduced between 5″ and 6″ whereas the (lower ionization) N^+ is being reduced only beyond 7.″5. C° increases by 60% in the interval from $\sim$4.″0 to $\sim$8.″5, Ca^+ by a slightly smaller fraction.

We find the conclusions about the ionization in HH 255 so surprising that we would like to confirm these results even further. It might seem obvious that one way to do this would be to study the "nebular" line ratio of [O II]/[O I] and [N II]/[N I]. This approach involves some problems. The nebular lines of [O II] have a considerably different excitation energy from those of [O I] (3.31 eV vs. 1.96 eV). The [N I] nebular lines have a very different transition probability from the [N II] lines (7×10^{-6} s^{-1} vs. 3×10^{-3} s^{-1}). So in both cases the line ratios will not be determined only by the ionization but to some extent also by the excitation. Nevertheless, we do not expect too drastic a change of the excitation because of the slowly varying electron density (see below; Fig. 6).

In Fig. 3 we have plotted the ratio of [O II]$\lambda\lambda$(3726 + 3729)/[O I]$\lambda\lambda$(6300 + 6363) and the ratio [N II]$\lambda\lambda$(6548 + 6583)/[N I]$\lambda\lambda$(5198 + 5200). The curves will probably to some extent be influenced by the different excitation of the lines but it is plausible that the main properties of the curves (and especially the large gradients) are caused by the variations in the degree of ionization as shown in Fig. 2. This expectation is confirmed by the properties of the [O II]/[O I] and [N II]/[N I] curves in Fig. 3. Both curves show again a very steep increase at 3″ (which must be the same sudden increase of general ionization which is visible in Fig. 2). The maximum ionization is reached at 3.″5 and 4.″0. From the region to $\sim$7.″5 the ionization is roughly constant. Beyond this point the ionization diminishes with a moderately strong gradient like the curves in Fig. 2.

We have established the rapid increase of the general ionization over a short distance scale from 2.″5 to 4.″0 (i.e. from 375 to 600 a.u., see Mundt 1985) from T Tau. This ionization increase

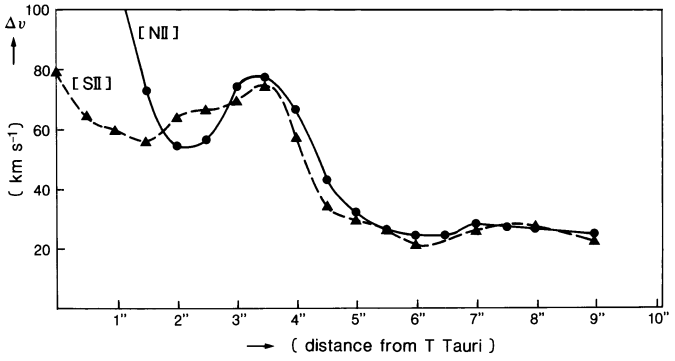

Fig. 4. The velocity dispersion (FWHM) for the [N II]λ6583 and the [S II]λ6731 line as a function of distance from T Tau for P.A. 180°. The position of the maximum of the velocity dispersion at 3.″5 agrees almost with the region of greatest change of ionization (3″, see Fig. 2). The estimated mean error for the velocity dispersion is $\sim$10 km s^{-1}.

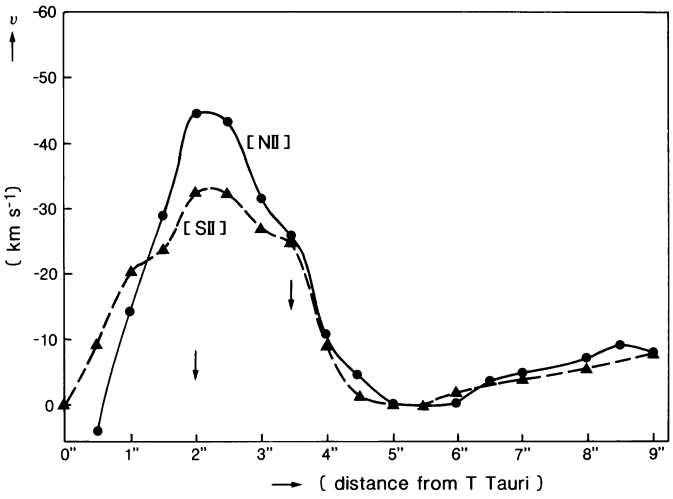

Fig. 5. The centroid radial velocity (with respect to the stellar photospheric velocity) for the [N II]λ6583 and [S II]λ6731 lines as a function of distance from T Tau for P.A. 180°. A maximum is reached at $\sim$2″. The steep decline begins at $\sim$3.″3 close to the greatest change of ionization (3″, see Fig. 2). At 4.″5 the value of $\sim$0 km s^{-1} is reached with a very small change for the rest of Burnham's nebula. The estimated mean error for the radial velocity is $\leq$5 km s^{-1}.

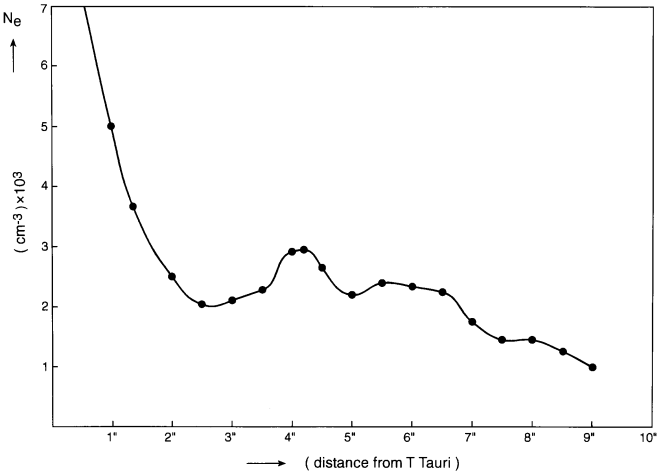

Fig. 6. The electron density N_e as a function of the distance from T Tau for P.A. 180°. For a distance between approximately 2″ and 7″ N_e varies only between 2×10^3 and 3×10^3 cm^{-3}. The N_e curve has a small maximum at 4″.

seems to occur for all elements which we could easily study, namely N, O, C and Ca. In the following we shall determine whether this ionization increase is coupled to drastic changes of the gas kinematics.

We study the dependence of the velocity dispersion Δv (FWHM) and the centroid radial velocity v with the distance from the star (Fig. 4 and Fig. 5). We discuss first the Δv. After a decrease of the velocity dispersion from the star to about 2″ there follows an increase and a secondary maximum at $\sim$3.″5. Both the [N II]λ6583 and the [S II]λ6731 reach a FWHM of $\sim$80 km s^{-1} at this point. After that there is a steep drop in the velocity dispersion. At 4.″5 the "asymptotic" value of $\Delta v \sim$ 25 km s^{-1} is almost reached. After that the Δv remains essentially unchanged at $\sim$25 km s^{-1}. It is important to note that the maximum of the velocity dispersion occurs at the same position where the maximum ionization is reached, recognizable by the fact that the [O III] emission has its maximum (3.″5). ([C I] reaches its minimum at about the same place.)

The relation between the centroid radial velocity and the ionization is slightly more complicated. As Fig. 5 shows, for both lines [N II]λ6583 and [S II]λ6731, the centroid radial velocity shows a maximum at $\sim$2.″0, a position which corresponds to the minimum in the velocity dispersion. There is a moderately steep decrease between 2.″5 and 3.″5. Beyond 3.″5 we find a very steep decrease from 3.″5 to 4.″5, practically reaching 0 km s^{-1} (the photospheric velocity) at 4.″5. This occurs in the region where approximately the ionization has reached its maximum. (the [Ca II] and the [C I] lines have a minimum at about this location.)

Finally, we have studied the distribution of the electron density N_e as a function of the distance from T Tau (Fig. 6). The electron density has been determined from the line ratio λ6716/λ6731 of [S II] (see, e.g., Aller 1984; Osterbrook 1989). T Tau is surrounded by a region of high density (Böhm & Solf 1994) which decreases very steeply outward up to a distance of 2.″5. At this distance (where the ionization starts to increase) N_e starts to increase and reaches a maximum at 4.″5 (see Fig. 2). It is to be expected the N_e has a maximum where the ionization has a maximum. However, a detailed explanation of Fig. 6 seems to be difficult, because the N_e distribution shown there seems to be at least composed of two density distributions with variable degree of ionization, a) the declining density distribution starting at the star and b) (starting at $\sim$2.″5?) the "shock wave" distribution.

4. Discussion

Our starting point for the discussion is the statement that Burnham's nebula (HH 255) is undoubtedly a Herbig-Haro object

(shown by Herbig 1951; Schwartz 1974, and especially by the strong and detailed evidence presented by Solf et al. 1988). Consequently we should expect that in the observationally determined kinematics and in the ionization stratification the presence of a shock wave is recognizable or at least that the observational results are compatible with a presence of a shock wave of sufficient strength.

If the shock wave is a bow shock like structure (as is true in many HH objects) then the "full width at zero intensity" (integrated over the object) is identical to the shock velocity, independent of the orientation of the bow shock (Hartigan et al. 1987). Often the full width at zero intensity is approximated by the full width at 10% intensity (FW0.1, see also Hartigan et al. 1987). In HH 255, in the region south of T Tau we see indications of the development of a shock wave excitation but the velocity dispersion in the region 4.″5 south of T Tau and beyond stays very small. The FWHM is $\sim$25 km s^{-1} or less (see Fig. 4) the derived FW0.1 is $\sim$40 km s^{-1}. This is considerably lower than the shock velocity of 90 km s^{-1} which is, at least, required to form the observed O^{++}. It would be helpful to see the spatial dependence of the FWHM of [O III]λ5007. However, there are no high-resolution spectra available in this wavelength range.

In this respect HH 255 behaves very different from other HH objects (see, e.g., Böhm 1995). In "normal" HH objects the measured velocity dispersion is usually larger, not smaller, than the shock velocity required by the observed ionization. (This is understandable, because some not yet known velocity distribution may have been added to the velocity distribution of a "pure" bow shock.) But (to the best of our knowledge) except for HH 255 there is no other HH object known for which the velocity derived from the ionization model is smaller than the shock velocity derived from the velocity dispersion.

At least as enigmatic as the low velocity dispersion is the centroid radial velocity which is in the main part of Burnham's nebula between 0 km s^{-1} and -7 km s^{-1} (with respect to the photosphere of T Tau; see Fig. 5). Especially in the region where the ionization is high the centroid radial velocity is practically exactly 0 km s^{-1}.

The conclusions from these two facts (the small velocity dispersion Δv and the zero centroid velocity) must be that the shock in HH 255 cannot even be approximated by a bow shock. The naive interpretation would be that we see (in the case of HH 255) essentially a plane shock edge-on, so that (by accident) the centroid radial velocity and the radial velocity dispersion appear small. We feel that this interpretation is not very convincing. Why should there be a plane shock wave close to a star ($\sim$500 a.u. from the star)? It is clear that in the assumed shock wave the kinematics stays approximately the same over a sizable distance. It has been shown earlier (Böhm & Solf 1994) that component E (see Fig. 1) shows basically the same kinematic properties along the P.A. 135° as along 180°. Especially the centroid radial velocity goes to zero in both cases. It is hard to imagine what would cause such a plane shock front (without visible boundary effects). It is even harder to imagine that this shock front would be oriented in such a way that the measured centroid radial velocity appears to be zero with respect to the star seen from us. The main objection against a plane shock seen edge-on, namely the large geometrical extent of the ionization zone, will be discussed below.

So far we have discussed mainly the kinematics of Burnham's nebula. Very important additional information comes from the close correlation between the kinematics and the observed properties of ionization discussed in the preceding section. Basically at the border between component D and E (Fig. 1) we found the following correlation between the almost discontinuous variation of the kinematics and of the degree of ionization (see Figs. 2–6).

At 2.″5 S of T Tau there starts a rapid increase of the velocity dispersion Δv (FWHM) which reaches a maximum of $\sim$80 km s^{-1} at 3.″5 and then declines very fast. At 2.″5 south of T Tau also the ionization sets in, first visible in the rapid increase of the ratio of [N II]/[O I] and in the rapidly increasing intensity of the [O III] lines (Fig. 2, see also Fig. 3). The ionization of O ($O^+ \longrightarrow O^{++}$) reaches its maximum at $\sim$3.″5 the same place at which Δv has its maximum. It seems that the rapid increase of the velocity dispersion may be causually related to the rapid onset of ionization. In that sense there are even qualitative similarities to a bow shock (see, e.g., Raga & Böhm 1985, 1986; Hartigan et al. 1987). However, the correlation of the velocities and the degree of ionization does not agree with this interpretation.

Of additional interest is the correlation of the centroid radial velocity (with respect to T Tau) and the electron density with the degree of ionization. The centroid radial velocity (Fig. 5) becomes more negative with the distance from T Tau, reaches -45 km s^{-1} at 2.″ from the star, between 2.″5 and 3.″5 the negative velocity decreases fairly steeply while at the same distance (see above) the velocity dispersion and the degree of ionization increases rapidly. Over the short distance between 3.″5 and 4.″5 the radial velocity decreases even more steeply and goes to 0 km s^{-1}. This happens at the same place where the velocity dispersion becomes very small and where the ionization has reached its maximum.

Finally, there is a correlation between the electron density N_e (Fig. 6) and the other quantities discussed here. Up to the point ($\sim$2.″5) where the velocity dispersion begins to increase, N_e decreases steeply with the distance from the star. At this point N_e begins to increase together with the velocity dispersion (Fig. 4) and the ionization (Fig. 2). While the velocity dispersion and the ionization reach their maximum at approximately 3.″5, the N_e maximum occurs at a slightly larger distance from the star. There seems to be a flat minimum in the N_e distribution at about the place where the centroid radial velocity has reached zero (Figs. 5, 6).

So far we have discussed the relation between the onset of ionization, the properties of the N_e distribution and the gas kinematics in the thin layer between 2.″5 and 4.″5 S of T Tau. In this region we find rapid changes in the kinematics and a drastic increase of ionization from low to fairly high values. In a purely qualitative way the results discussed so far seems to make sense for the generation of ionization by a supersonic hydrodynamic

flow. We see a relatively ordered flow (with centroid velocity and velocity dispersion being about equal) converted into a flow of increased velocity dispersion and with the centroid velocity going down to zero. This region has some vague similarity to the stagnation region of a bow shock (see the theoretical position-velocity diagrams calculated by Raga and Böhm 1985, 1986) or it may be a region of supersonic turbulence (whose details are not fully understood) created by a shock wave.

The fundamental difficulty arises when we consider the great extent of the ionization zone. The ionization generation at a distance between 2.″5 and 3.″5 from the star seems to persist to at least 9" from the star. Assuming a distance to T Tau of ∼140 pc (see, e.g., Kenyon, Dobrzycka & Hartmann 1994, Mundt 1985) the ionization zone covers approximately 900 a.u. This clearly excludes the interpretation which we considered briefly above: If we would see a plane shock edge-on (making this assumption in order to explain the fact that we essentially have only a centroid velocity of 0 km s^{-1} beyond 4.″5) we would, even for a pre-shock particle density as low as 100 cm^{-3}, obtain a thickness for the visible shock of only 10 a.u. (corresponding to 0.″07). Over this thickness the ionization would disappear again. This is a factor 100 smaller than the thickness of the observed ionization stratification. A plane shock seen edge-on is therefore completely excluded as an explanation of the zero-velocity in the ionization zone. Since we can also exclude a bow shock structure (see above) the character of the shock wave in Burnham's nebula remains an unsolved problem.

Presently further observational studies of the jet outflows from T Tau are in press or in preparation. One may hope that they will in the future contribute to the solution of the problems discussed here. We mention specifically the discovery of a very large bipolar outflow from T Tau, whose extent is 1.5 pc (Reipurth, Bally & Devine in preparation). It is oriented NNW to SSE (similar to the components C and D of the bipolar outflow described by Böhm and Solf 1994). Furthermore there are now high-resolution studies of molecular H_2 by Herbst et al. (1996) and by Zinnecker & Quirrenbach (in preparation).

5. Conclusions

We find in Burnham's nebulae a drastic change of the velocity dispersion, the centroid radial velocity, the degree of ionization and the electron density in a very narrow range between 2.″5 and 4.″5 S of T Tau. (Most of the changes occurs in an even narrower range between 2.″5 and 3.″5.) In this region the velocity dispersion shows a steep maximum and declines to very small values, the centroid radial velocity goes to zero with respect to the star, and the degree of ionization rises very steeply over a surprisingly short distance. It seems that the supersonic hydrodynamics which occurs in these regions causes the steep increase in ionization. However, the long persistence of rather high ionization (over a distance of at least ∼900 a.u.) contradicts the predictions for the typical shock wave models used in other HH objects (although the ratios of the total fluxes of the different lines in HH 255 agree very well with the shock wave predictions). The optically emitting region can neither be explained as a bow shock nor as a plane shock wave seen "side-on". The fact that component E (designation by Böhm & Solf 1994), the main part of HH 255, has a centroid radial velocity of ∼0 km s^{-1}, and in the same region a very low velocity dispersion, offers serious problems for any detailed shock wave interpretation. The remote possibility that we have a standing shock wave has to be further investigated. Our studies strongly confirm the possibility discussed by Böhm & Solf (1994) that component E (Fig. 1) is somehow caused by the hydrodynamic interaction between component D and component E and that this interaction leads to very abrupt changes at ∼3″ south of T Tau.

Acknowledgements. We thank the referee, Bo Reipurth, for a very careful reading of the paper and helpful comments.

References

Aller, L. H., 1984, *Physics of Thermal Gaseous Nebula* (Dordrecht: Reidel)
Böhm, K.H., 1995, in *Shocks in Astrophysics*, Contributions to the Conference held in Manchester, eds. T. Miller & A. C. Raga (Dordrecht: Kluwer), p. 11
Böhm, K.H. & Solf, J., 1994, ApJ 430, 277
Bührke, T., Brugel, E. W. & Mundt, R., 1986, A&A 163, 83
Burnham, S. W., 1894, Pub. Lick Obs. 2, 175
Hartigan, P., Raymond, J. & Hartmann, L., 1987, ApJ 316, 323
Herbig, G. H., 1950, ApJ 111, 11
Herbig, G. H., 1951, ApJ 113, 697
Herbst, T. M., Beckwith, S. V. W., Glindemann, A., et al., 1996, AJ 111, 2403
Hirth, G. A., 1994, Ph.D. Thesis, University of Heidelberg
Hirth, G. A., Mundt, R. & Solf, J., 1994, A&A 285, 233
Kenyon, S. J., Dobrzycka, D., & Hartmann, L., 1994, AJ 108, 1872
Kwan, J. & Tademaru, E., 1988, ApJ 332, L41
Kwan, J. & Tademaru, E., 1995, ApJ 454, 382
Mundt, R., 1985, in *Protostars and Planets II*, ed. D. C. Black and M. S. Matthews (The University of Arizona Press, Tucson), p. 414
Osterbrock, D. E., 1958, PASP 70, 399
Osterbrock, D. E., 1989, *Astrophysics of Gaseous Nebulae and Galactic Nuclei* (Mill Valley: Univ. Science Books)
Raga, A. C. & Böhm, K.H., 1985, ApJS 58, 201
Raga, A. C. & Böhm, K.H., 1986, ApJ 308, 829
Reipurth, B., 1994, *A general catalogue of Herbig-Haro objects*, electronically published via ftp.hq.eso.org in directory /pub/catalogs/Herbig-Haro
Schwartz, R. D., 1974, ApJ 191, 419
Schwartz, R. D., 1975, ApJ 195, 631
Solf, J., 1989, in *Low Mass Star Formation and Pre-Main Sequence Objects*, ed. B. Reipurth (ESO Conf. Proc. 33, Garching), 399
Solf, J., 1993, in *Stellar and Circumstellar Astrophysics*, ed. G. Wallerstein and A. Noriega-Crespo (A.S.P. Conference Series, San Francisco), p. 22
Solf, J. & Böhm, K.H., 1993, ApJ 410, L31
Solf, J., Böhm, K.H. & Raga, A. C., 1988, ApJ 334, 229
Staude, H. J. & Elsässer, H., 1993, A&AR 5, 165

This article was processed by the author using Springer-Verlag LaTeX A&A style file *L-AA* version 3.